Supporting Information for: **Kinetics of Thermal Unfolding of Phenylalanine Hydroxylase Containing Different Metal Cofactors (Fe^{II}, Co^{II}, and Zn^{II}) and Their Isokinetic Relationship**

Aristobulo Loaiza[a], Kathryn M. Armstrong[b], Brian M. Baker[b] and Mahdi M. Abu-Omar[a]*

[a] Brown Laboratory, Department of Chemistry, Purdue University, 560 Oval Drive, West Lafayette, Indiana 47907, USA

[b] Department of Chemistry and Biochemistry, University of Notre Dame, Notre Dame, Indiana 46556, USA

Table of Contents

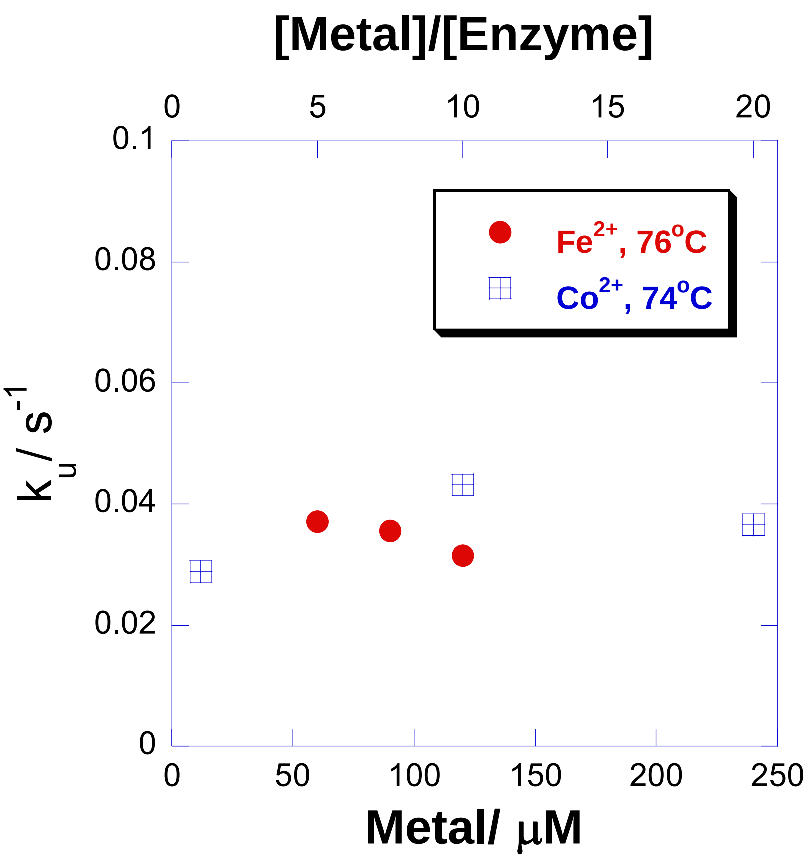

Figure S1. Metal-dependence of holo-cPAH thermal unfolding rate. Thermal unfolding rate constants as a function of metal concentration and metal:enzyme (M/E), ● represents unfolding rates of Fe-cPAH at 76˚C, and ⊞ represents unfolding rates of Co-cPAH at 74˚C.

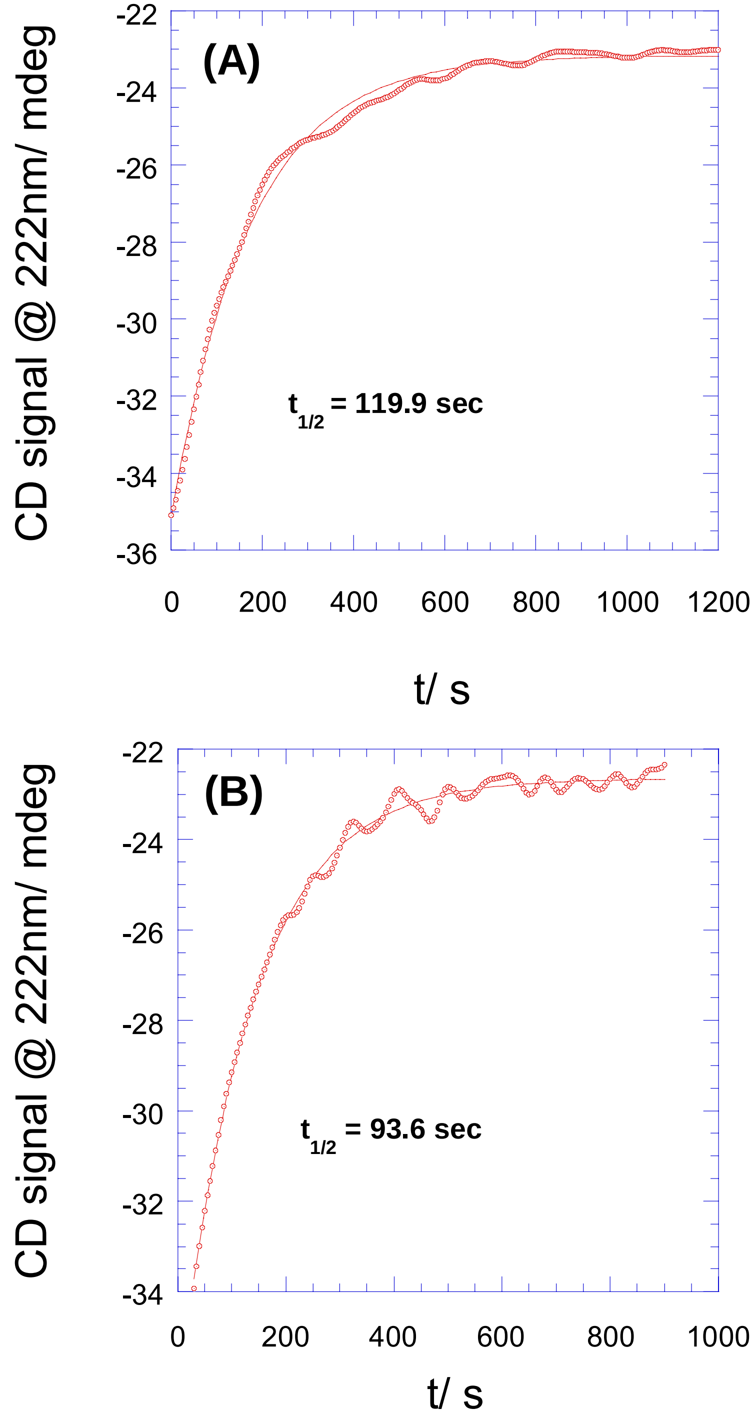

Figure S2. Kinetic profiles for the thermal unfolding of Zn-cPAH (20 µM). A, Thermal unfolding at 58˚C with corresponding unfolding reaction half-life ($t_{1/2}$). B, Thermal unfolding at 60˚C.

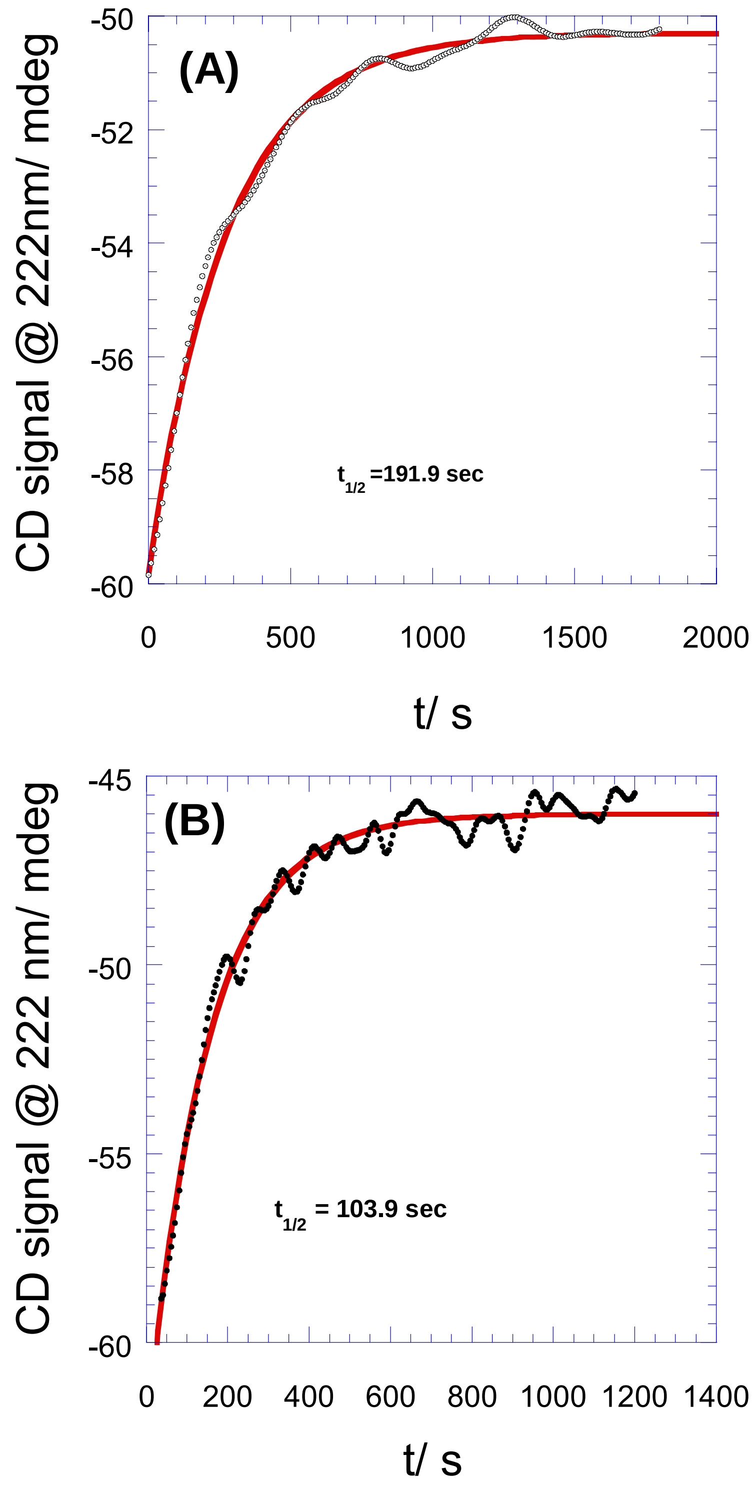

Figure S3. Kinetic profiles for the thermal unfolding of apo-cPAH (20 μM). A, Thermal unfolding at 46˚C with corresponding unfolding reaction half-life ($t_{1/2}$). B, Thermal unfolding at 50˚C.

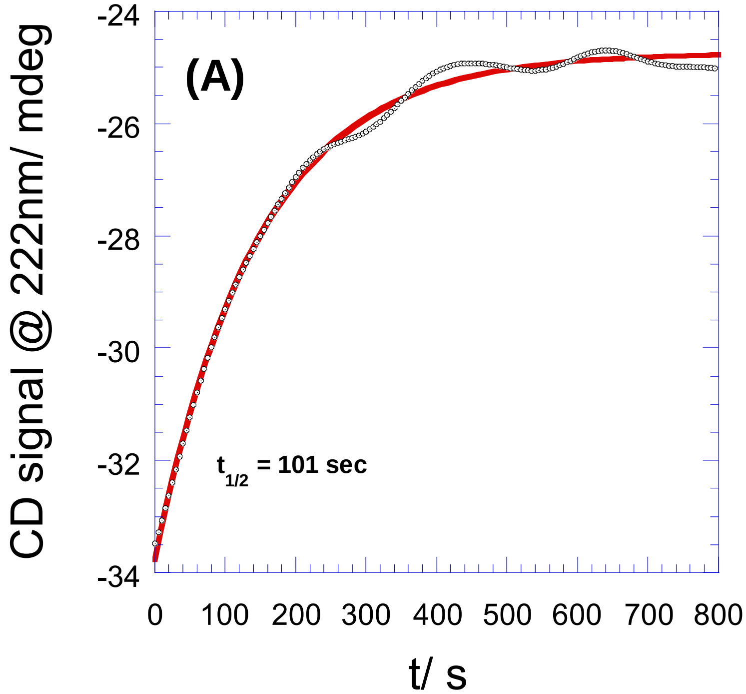

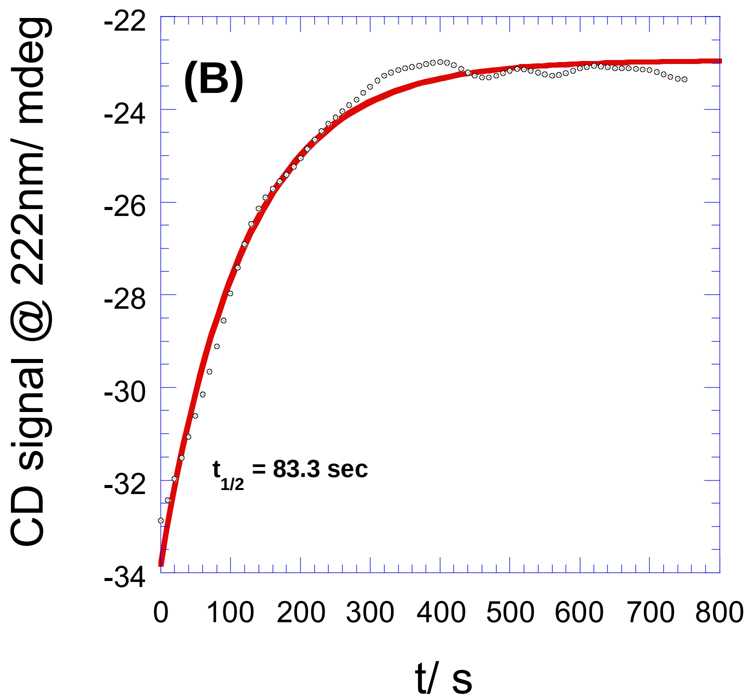

Figure S4. Kinetic profiles for the thermal unfolding of Fe-cPAH (20 μM). A, Thermal unfolding at 56˚C with corresponding unfolding reaction half-life ($t_{1/2}$). B, Thermal unfolding at 60˚C.

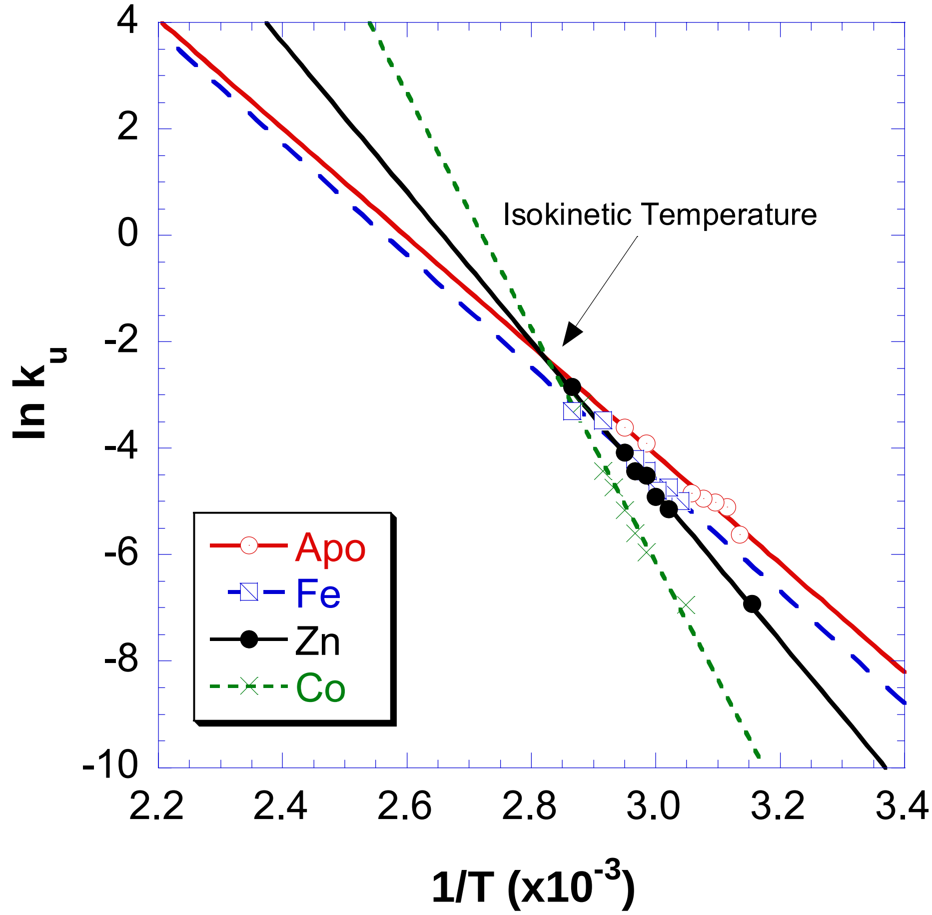

Figure S5. Arrhenius plots of apo- and holo-cPAH.

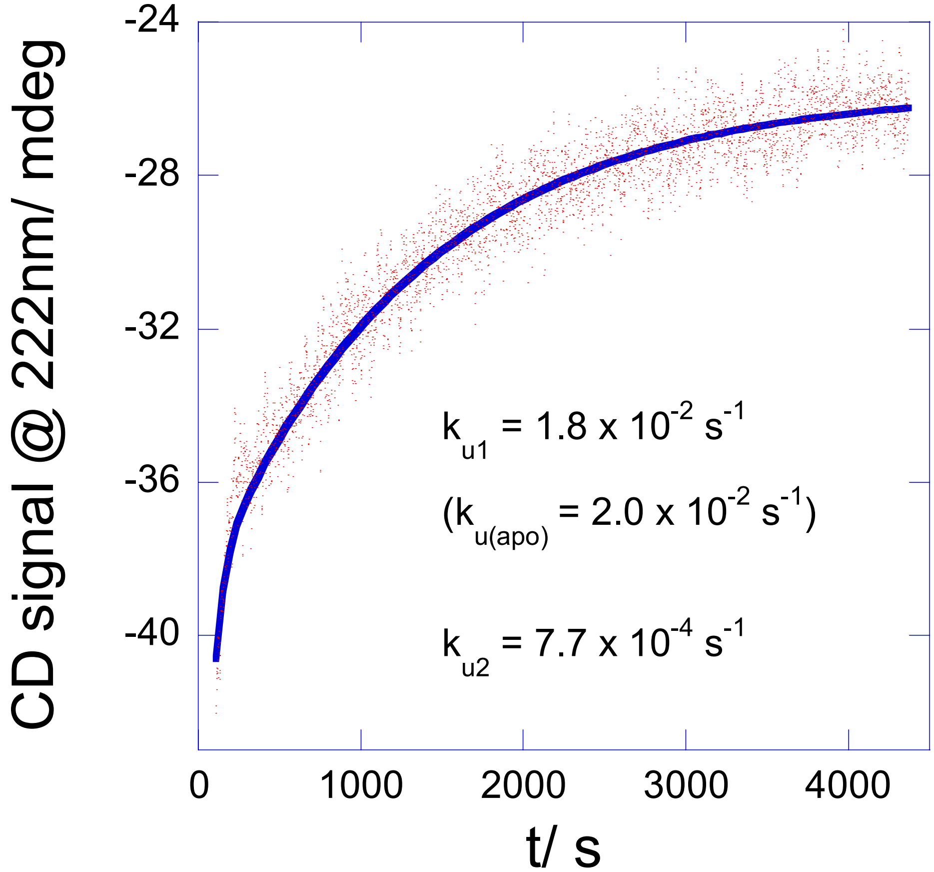

Figure S6. Biphasic unfolding kinetics of Co-cPAH using sub-stoicheometric [Co^{2+}]. Biphasic unfolding kinetics of Co-cPAH at 62°C fitted two a bi-exponential (blue curve), which yield two unfolding rate constants k_{u1} and k_{u2} . Unfolding rate constant for apo at 62°C is shown in parenthesis.

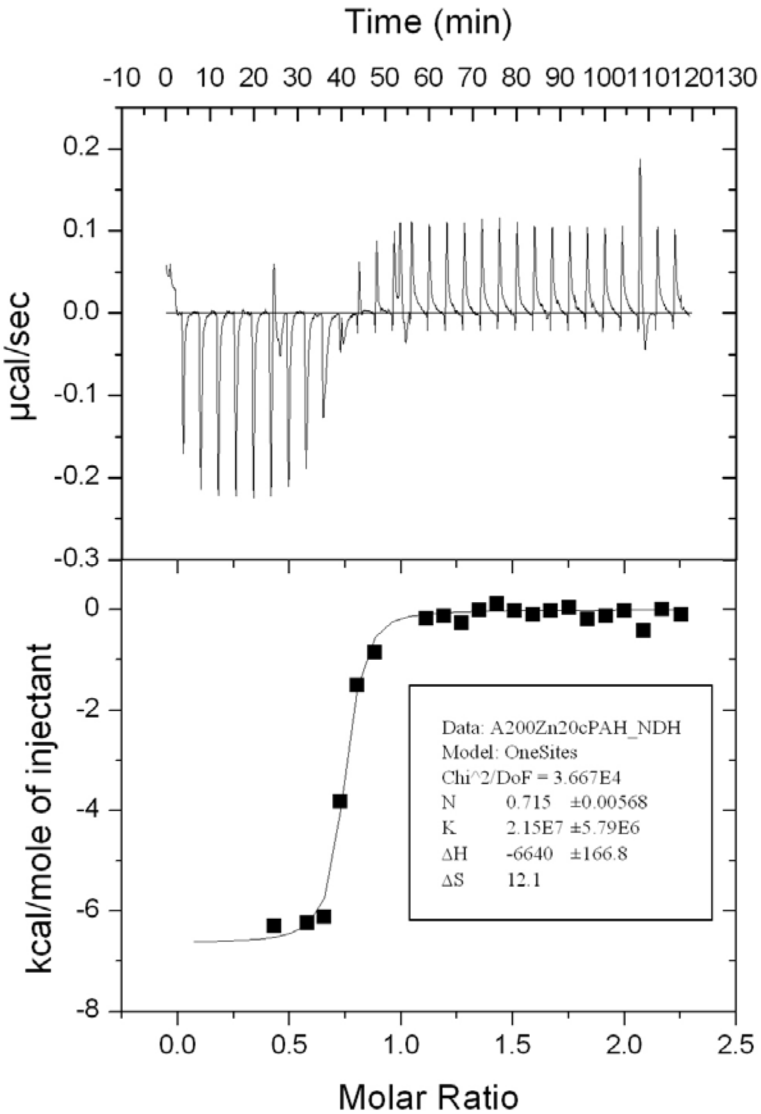

Figure S7. Calorimetric trace (upper panel) for titration of 200 μM $ZnCl_2$ into 20 μM apo cPAH in 50 mM Hepes pH 7.44 at 37 °C. Inset, binding constant (K_a) in M^{-1},thermodynamic parameters (ΔH_{ITC}, ΔS_{ITC}) in cal mol^{-1} and cal mol K^{-1}, and stoichiometry (N_{ITC}). Lower panel, plot of the net heat released as a function of the ratio of $ZnCl_2$ to apo-cPAH. Solid line represents single site binding model fit (See materials and methods).

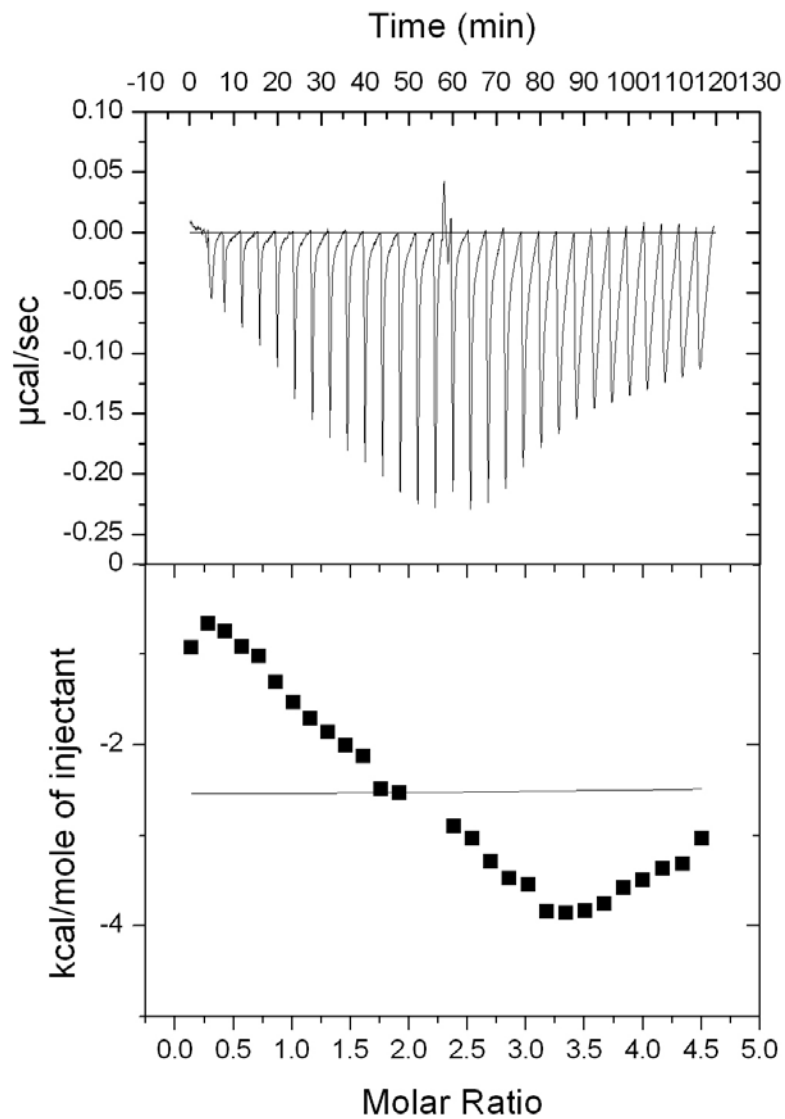

Figure S8. Calorimetric trace (upper panel) for titration of 400 μM $Fe(NH_3)SO_4$ into 20 μM apo cPAH in 50 mM Hepes pH 7.44, with 2.5 mM TCEP at 37 °C. Lower panel, plot of the net heat released as a function of the ratio of $Fe(NH_3)SO_4$ to apo-cPAH.

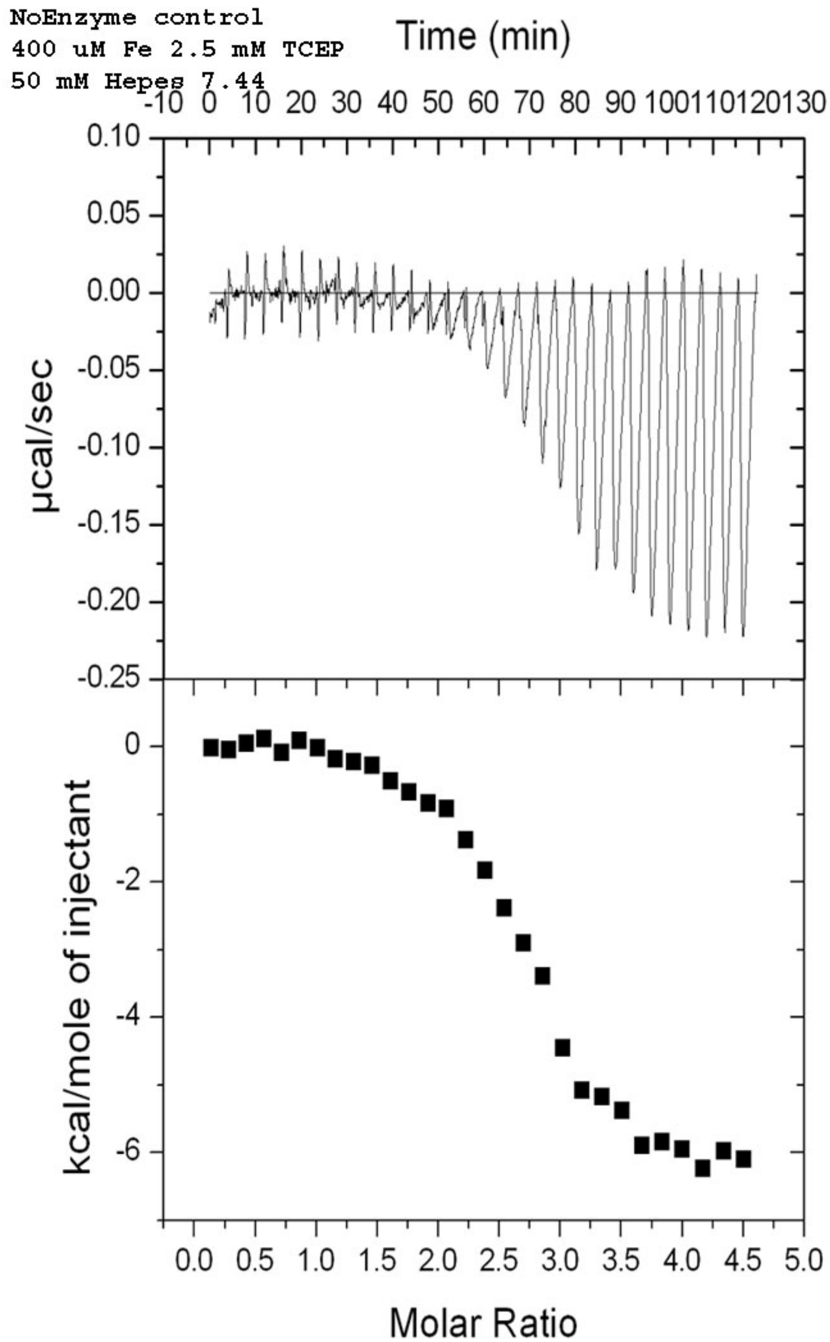

Figure S9. No enzyme control Titration**.** Calorimetric trace (upper panel) for titration of 400 μM $Fe(NH_3)SO_4$ in 50 mM Hepes pH 7.44 with 2.5 mM TCEP into 50 mM Hepes pH 7.44, with 2.5

mM TCEP at 37 °C.Lower panel, plot of the net heat released as a function of the ratio of $Fe(NH_3)SO_4$ to 50 mM Hepes buffer.

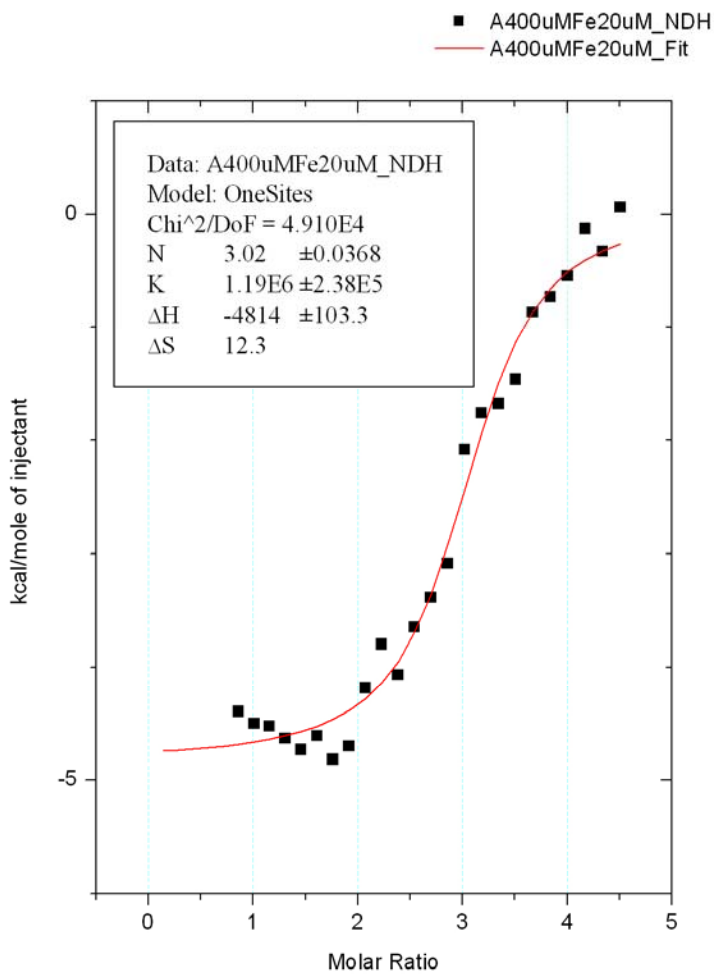

Figure S10. Enthalpic trace resulting from the subtraction of figure S9 enthalpic data from Figure S8 enthalpic data. Inset, binding constant (K_a) in M^{-1},thermodynamic parameters (ΔH_{ITC}, ΔS_{ITC}) in cal mol^{-1} and cal mol K^{-1}, and stoichiometry (N_{ITC}). Solid line represents single site binding model fit (See materials and methods).

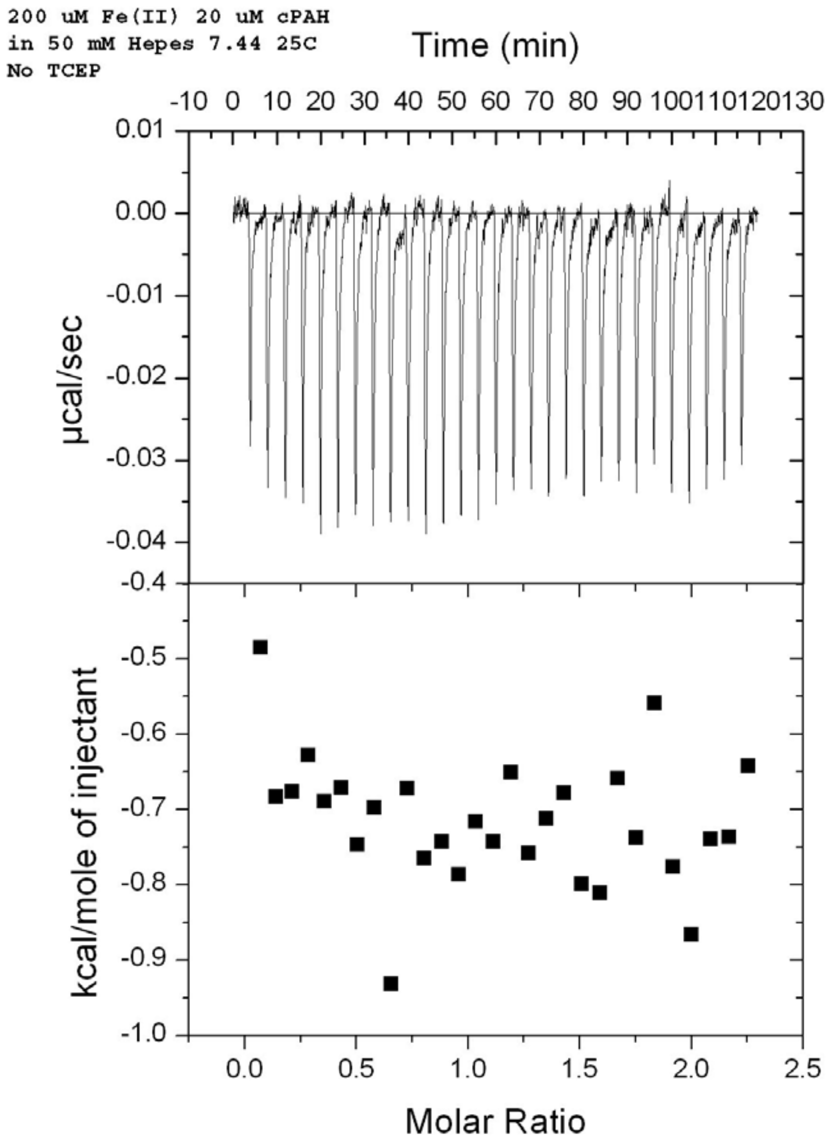

Figure S11. Calorimetric trace (upper panel) for titration of 200 μM $Fe(NH_3)SO_4$ into 20 μM apo cPAH in 50 mM Hepes pH 7.44, without TCEP. Lower panel, plot of the net heat released as a function of the ratio of $Fe(NH_3)SO_4$ to apo-cPAH.